Princeton Plasma Physics Laboratory

PPPL- 4609

PPPL- 4609

Electromagnetic Transport From Microtearing Mode Turbulence

W. Guttenfelder, J. Candy, S.M. Kaye, W.M. Nevins, E. Wang, R.E. Bell, G.W. Hammett,
B.P. LeBlanc, D.R. Mikkelsen, and H. Yuh

March, 2011

Prepared for the U.S. Department of Energy under Contract DE-AC02-09CH11466.

Princeton Plasma Physics Laboratory
Report Disclaimers

Full Legal Disclaimer

Trademark Disclaimer

PPPL Report Availability

Princeton Plasma Physics Laboratory:

http://www.pppl.gov/techreports.cfm

Office of Scientific and Technical Information (OSTI):

http://www.osti.gov/bridge

Related Links:

U.S. Department of Energy

Office of Scientific and Technical Information

Fusion Links

Electromagnetic transport from microtearing mode turbulence

W. Guttenfelder[1], J. Candy[2], S.M. Kaye[1], W.M. Nevins[3], E. Wang[3], R.E. Bell[1], G.W. Hammett[1], B.P. LeBlanc[1], D.R. Mikkelsen[1], H. Yuh[4]

[1]*Princeton Plasma Physics Laboratory, Princeton NJ 08543*
[2]*General Atomics, San Diego, CA 92186*
[3]*Lawrence Livermore National Laboratory, Livermore, CA 94551*
[4]*Nova Photonics Inc., Princeton, NJ 08540*

This Letter presents non-linear gyrokinetic simulations of microtearing mode turbulence. The simulations include collisional and electromagnetic effects and use experimental parameters from a high beta discharge in the National Spherical Torus Experiment (NSTX). The predicted electron thermal transport is comparable to that given by experimental analysis, and it is dominated by the electromagnetic contribution of electrons free streaming along the resulting stochastic magnetic field line trajectories. Experimental values of flow shear can significantly reduce the predicted transport.

PACS numbers: 52.35.Ra, 52.55.Fa, 52.65.Tt

The scaling of normalized energy confinement time with collisionality in spherical tokamaks (STs), $\Omega_i\tau_E \sim \nu_*^{-(0.7\text{-}0.9)}$ [1,2] is favorable for extrapolation to next generation devices at lower ν_*. The microtearing mode [3,4] is often predicted to be unstable in neutral beam heated ST experiments [5-7] with a linear growth rate that scales consistent with the measured confinement trends ($\gamma_{lin} \sim \nu_e$). It is therefore an obvious candidate for describing transport in at least some ST plasmas. This Letter presents first-of-a-kind nonlinear gyrokinetic microtearing mode simulations which predict transport comparable to experimental results in the National Spherical Torus Experiment (NSTX).

Microtearing modes are small scale tearing modes with large toroidal (n) and poloidal (m) mode numbers. Theoretically they are driven unstable by having an electron temperature gradient ∇T_e projected onto helically-resonant radial perturbations of magnetic field lines, δB_{mn}, with a rational value of the safety factor, q=m/n. The parallel component of ∇T_e can drive a resonant parallel current (which reinforces δB_{mn} via Ampere's law) through multiple mechanisms, such as the thermal force [3] or interaction between the trapped/passing boundary layer [4], both requiring finite collisionality. The existence and strength of the instability will therefore depend on collisionality and electron beta (from Ampere's law). In the cylindrical limit, a single resonant mode can reconnect [8] and cause a magnetic island of width $w_{island} = 4\sqrt{\delta B / B_0 \cdot rR / ns}$ to form, where B_0 is the equilibrium field strength, R (r) is the major (minor) radius and $s=r/q\cdot q'$ is the magnetic shear. If the single-mode island width becomes larger than the separation between rational surfaces, $\Delta r_{rat}=1/nq'=1/k_\theta s$ ($k_\theta=nq/r$), stochasticity is expected to develop [9] which can cause rapid transport of electrons following the perturbed fieldline trajectories [10]. If many toroidal modes are present (separated by Δn) the minimum distance between adjacent resonant surfaces is $\delta r_{rat} \approx \Delta n/n^2 q'$. Therefore the island overlap criterion for stochasticity onset is more easily satisfied, especially for higher n. Evaluating this condition requires the amplitude of the saturated δB perturbations. The quasi-linear approximation $\delta B/B \approx \rho_e/L_{Te}$ [11] was used along with a collisional test-particle stochastic transport model [10] to model an NSTX discharge, giving quantitative agreement [7]. But the analytic χ_e expression does not follow the scaling of the linear instability, and it is extremely

sensitive to T_e and ∇T_e. It is unclear whether these scalings are expected to hold from non-linear turbulence simulations.

To provide a first principles prediction of the nonlinear magnetic perturbations δB and corresponding transport this Letter describes a set of non-linear gyrokinetic simulations for a discharge in NSTX that is unstable to only the microtearing mode. The simulations require resolving all rational surfaces in the computational domain to achieve saturation, and the transport is almost entirely electromagnetic as a result of stochastic field line trajectories. The predicted electron heat flux is close to experimental levels illustrating microtearing turbulence can be important in spherical tokamaks.

The simulations are based on NSTX discharge 120968 (B_T=0.35 T, I_p=0.7 MA, P_{NBI}=4 MW, R/a=0.82 m/0.62 m) that is common to confinement studies that scale plasma current, magnetic field and dimensionless collisionality and beta [1,12]. Linear stability analysis using the Eulerian gyrokinetic code GYRO [13] finds that the microtearing mode is the only ion scale ($k_\theta\rho_s<1$, where $\rho_s=c_s/\Omega_i$, $c_s=(T_e/m_i)^{1/2}$, $\Omega_i=Z_ieB/m_i$) instability in the outer half radius (r/a=0.5-0.8) while the smaller scale electron temperature gradient (ETG) instability ($k_\theta\rho_s>>1$) is unstable only farther out (r/a≈0.8). Fig. 1a shows that microtearing modes at r/a=0.6 are unstable for $k_\theta\rho_s\leq1.05$, or n≤50 (m≤85, q=1.69). Compressional magnetic perturbations ($\delta B_{||}$) have little influence on the growth rate and structure of this mode and are neglected in the nonlinear simulations.

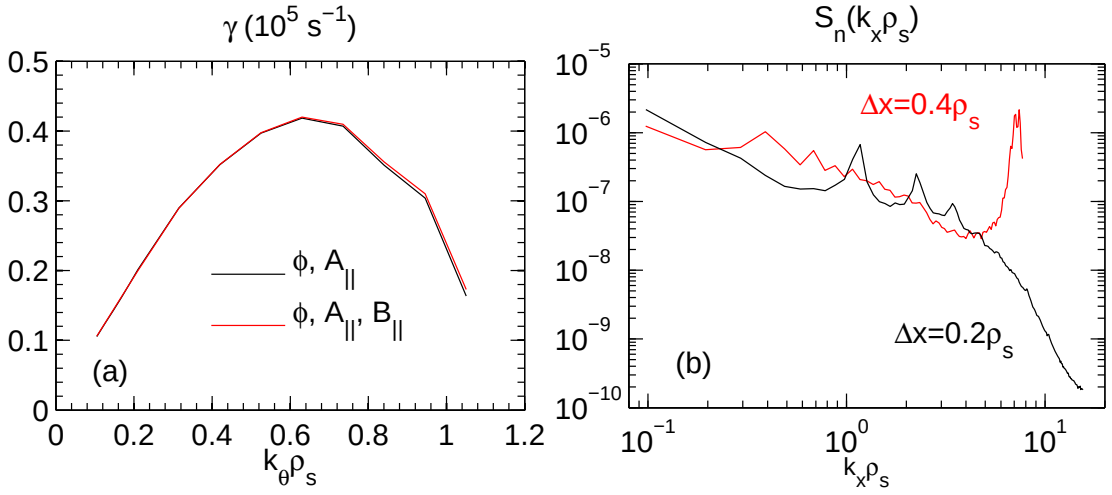

Fig. 1. (a) Converged linear microtearing spectra with and without compressional magnetic perturbations, ($B_{||}$). (b) Density power spectrum vs. k_x for $\Delta x=0.2\ \rho_s$ and $0.4\ \rho_s$.

While the microtearing mode in highly shaped, high beta ST plasmas does not always follow more simple theoretical limits [6], gyrokinetic calculations demonstrate the mode requires sufficient beta, collisionality, electron temperature gradient ($a/L_{Te}=-a/T_e\cdot\nabla T_e$), and positive magnetic shear to become linearly unstable. At r/a=0.6 in this NSTX discharge the microtearing mode dominates over all other micro-instabilities for a wide range of ν, β and a/L_{Te}. This location is therefore ideal for studying pure microtearing mode driven turbulence.

The linear modes exhibit narrow resonant parallel current perturbations ($\delta j_{||}$) centered on the rational surfaces and almost radially uniform magnetic perturbations. For the most unstable mode at $k_\theta\rho_s=0.63$ (n=30), the current channel width is $\Delta_j\approx 0.3\ \rho_s$, or ~1/3 of the rational surface separation $\Delta r_{rat}=0.9\ \rho_s$ (s=1.75). The corresponding density and potential fluctuations are also narrow and out of phase, very close to an unmagnetized (or adiabatic) ion response, $\delta n/n=-(e\delta\varphi/T)$. As a result of the narrow current channel, fine radial resolution ($\Delta x\approx 0.03\ \rho_s$) is required to obtain quantitative convergence in the linear growth rate. It is computationally prohibitive (and typically unnecessary) to use such high resolution required for linear convergence in a non-linear turbulence simulation. However, the microtearing mode depends explicitly on the presence of resonant current perturbations for instability to occur, so it is important to determine the minimum required Δx such that the current channel is resolved for each rational surface. In the present case, for the n=30 mode, this is satisfied for $\Delta x=0.2\ \rho_s$. The resulting structure is qualitatively identical to the converged linear result but with a growth rate that is ~15% smaller. Using a coarser resolution ($\Delta x=0.4\ \rho_s$) no longer allows for the mode to properly distinguish each rational surface and the resulting instability takes on a completely different (non-physical) appearance.

Guided by the discussion above, local nonlinear GYRO simulations were run (with fixed boundary conditions) with perpendicular dimensions $L_x\times L_y=80\times 60\ \rho_s$ using eight complex toroidal modes up to n=35 ($k_\theta\rho_s=0,0.105,\ldots,0.735$) and 400 radial grid points, allowing for all rational surfaces in the simulation domain to be resolved, $\Delta x\approx\min[\Delta r_{rat}]/4$. All other grid parameters were kept identical to the converged linear calculations, which use numerical equilibrium reconstruction [14] and physical parameters from experimental measurements ($a/L_{Te}=2.7$, $a/L_{Ti}=2.4$, $a/L_n=-0.8$, $T_e/T_i=1.06$). Two kinetic species are included (electrons and main deuterium ions at full mass ratio, $m_i/m_e=3600$), with finite electron collisionality

(ν_{ei}=1.49c_s/a, Z_{eff}=2.9) and electromagnetic perturbations ($\delta A_{||}$, $\beta_e=8\pi n_e T_e/B^2$=8.8%), using 8 energies, 12 pitch angles (2 signs of velocity), and 14 parallel orbit times. The resulting baseline simulation is statistically stationary for a duration longer than 800 a/c_s (using a time step Δt=0.002 a/c_s), with no indication of numerical instability. An important verification that these non-linear simulations are in fact sufficiently resolved is shown by the monotonically decaying tail in the density radial wavenumber power spectra shown in Fig. 1b (integrated over k_θ and averaged over the last 500 a/c_s). Conversely, with half the radial resolution (Δx=0.4 r_s), the power spectra for δn (and $\delta j_{||}$) have the non-physical appearance of being severely aliased (similar to unpublished simulations [15] using GS2 [16]) and the resulting transport is about five times larger. The dramatic change in nonlinear spectra in Fig. 1b supports the linear resolution analysis discussed previously.

Consistent with the broad spectra in Fig. 1b, the density perturbations for the saturated simulation are radially narrow (Fig. 2a) and elongated in the poloidal direction, with average correlation lengths $L_x \approx 0.7\ \rho_s$ and $L_y \approx 4\ \rho_s$. The structure of the density (and similar potential) perturbations is in stark contrast to the larger, isotropic density structures present in ion scale ITG/TEM turbulence ($L_x \approx L_y \approx 7\ \rho_s$) or the radially elongated eddies at much smaller dimension in ETG turbulence ($L_x/3 \approx L_y \approx 0.15\ \rho_s$). On the other hand, the magnetic perturbations ($\delta A_{||}$) are very broad with some instantaneous eddies stretching across the entire simulation domain (Fig. 2b).

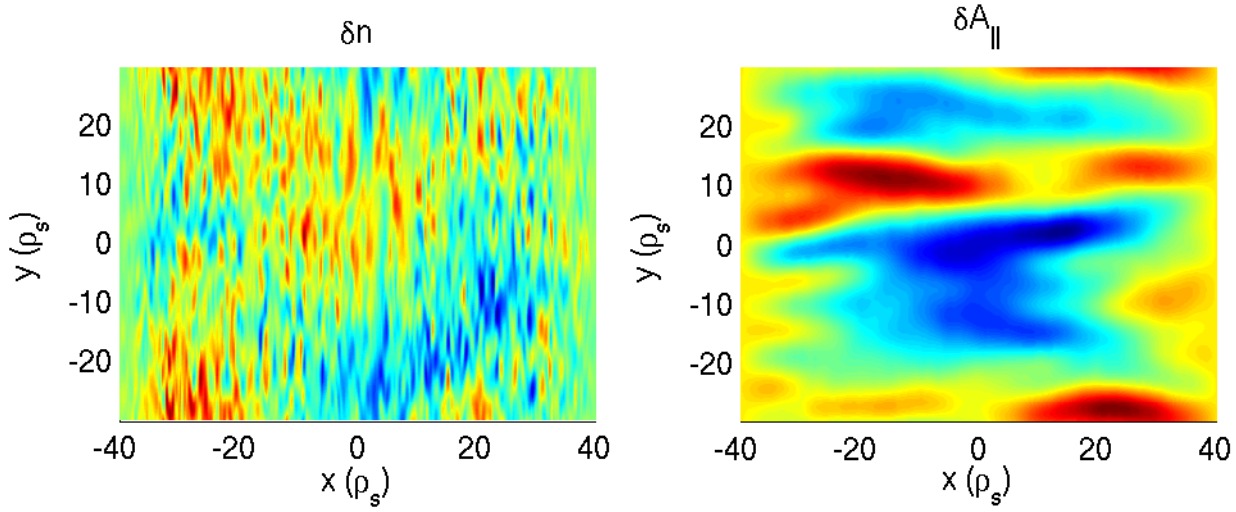

Fig. 2. Contour plots of (a)δn and (b)$\delta A_{||}$ perturbations at a snapshot in time.

We emphasize that the narrow radial extent of the density perturbations is a remnant of the underlying microtearing mode structure and is not due to the presence of strong, non-linearly generated n=0 zonal flows [17] as the averaged rms zonal flow shear rate, $\langle \omega_s^2 \rangle_{x,t}^{1/2} \approx 0.01\ c_s/a$ ($\omega_s = 1/B \cdot d^2(\delta\varphi)/dx^2$) is substantially smaller than the decorrelation rate of the electrostatic perturbations ($\Delta\omega_\varphi \approx 0.6\ c_s/a$). We also note that the perturbed magnetic shear resulting from the zonal $A_\parallel$ perturbations ($\tilde{s} = qR/B \cdot d(\delta B_y)/dx$) [18] is relatively small, $\langle \tilde{s}^2 \rangle_{x,t}^{1/2} \approx 0.1$ compared to the equilibrium magnetic shear (s=1.75), and is therefore not expected to be important in the saturation process. For reference, the average rms intensities of non-zonal components (n>0) are approximately $\delta n/n \approx e\varphi/T_e \approx 0.6\%$ and $\delta A_\parallel / c_s T_e \approx 0.4\%$.

The predicted electron thermal diffusivity in gyro-Bohm units is $\chi_e \approx 1.2 \cdot \rho_s^2 c_s/a$, corresponding to $\chi_e = 6\ m^2/s$. This is within the uncertainty of the experimental value $\chi_{e,exp} \approx 5\text{-}8\ m^2/s$ [1,12], confirming that microtearing mode driven turbulence can indeed cause significant electron thermal transport in NSTX. A unique feature of this simulation is that the electron heat flux is dominated entirely by the electromagnetic 'flutter' component ($\chi_{e,em}/\chi_{e,tot} > 98\%$). Again, this is in contrast to almost all other published gyrokinetic turbulence simulations, with the exception of cases very near the ideal or kinetic ballooning mode thresholds where $\chi_{e,em}/\chi_{e,tot}$ can reach values of 50-90% [18-20]. As discussed in the introduction, the transport from microtearing modes is expected to be a consequence of island overlap leading to stochastic field line trajectories. To test this, we compare the island widths estimated using the saturated magnetic spectra, $w_{island} \sim (\delta B_r/n)^{1/2} \sim \delta A_\parallel^{1/2}$, with the minimum separation in rational surfaces, δr_{rat}. Fig. 3 shows that the island overlap criteria $w_{island}(n) > \delta r_{rat}(n;\Delta n=5)$ [9] is satisfied above $k_\theta \rho_s > 0.21$ (n>10), approaching $w_{island}/\delta r_{rat} = 8$ at the highest toroidal mode number. As a result, the perturbed field line trajectories are stochastic throughout the entire simulation domain, illustrated by Poincare surface-of-section plots [21]. Following Rechester-Rosenbluth [10] a magnetic diffusivity

$$D_m = \frac{1}{N} \sum_{i=1}^{N} \lim_{\ell \to \infty} \frac{\left[r_i(\ell) - r_i(0) \right]^2}{2\ell} \qquad (1)$$

is calculated [21] to be $D_m = 6 \times 10^{-7}$ m from an ensemble of N=100 perturbed trajectories, $r_i(\ell)$, intergrated for 3000 poloidal transits. As the electron mean free path ($\lambda_{mfp} = 12.5$ m) is much longer than the magnetic correlation length [10] $L_c = \pi R/\ln(0.5\pi s) \approx 2.5$ m, a collisionless

stochastic transport estimate can be made using the model equation $\chi_{e,st} = 2\sqrt{2/\pi} \cdot f_p D_m v_{Te}$ [10,21,22], where $v_{Te}=(T_e/m_e)^{1/2}$ and $f_p=63\%$ is the fraction of passing particles expected to follow the perturbed trajectories. The use of f_p is validated by the fact that >70% of the calculated transport comes from passing particles, mostly with energy $E>2T_e$, i.e. particles with the largest parallel velocity. The resulting model prediction, $\chi_{e,st}=0.92\ \rho_s^2 c_s/a$, is within 25% of the simulation, providing strong evidence that the transport is dominated by electrons diffusing in a stochastic magnetic field.

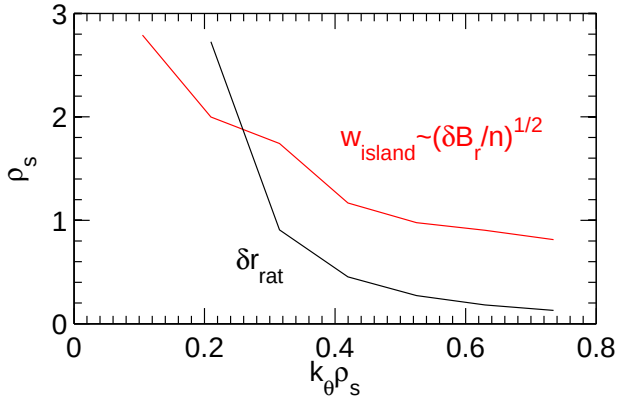

Fig. 3. Predicted island width at saturation and minimum separation of rational surfaces.

As indicated by the island widths in Fig. 3, the $\delta A_{\|}$ spectrum peaks at the lowest finite $k_\theta\rho_s$ modes. The peak in transport coincides with these modes and is noticeably down-shifted to wavelengths longer than the maximum linear growth rate, $(k_\theta\rho_s)_{lin,max}=0.63$ (Fig. 1a), as predicted to occur in the non-linear theory of Drake et al. [11]. This theory also predicts a saturated amplitude $\delta B_r/B=\rho_e/L_{Te}=0.065\%$, within a factor of ~2 of the simulation result ($\delta B_r/B=0.15\%$), partially validating the transport model utilized in previous NSTX transport modeling [7]. The fact that the magnetic fluctuations are strongest at the lowest finite toroidal modes is also apparent in the density spectra in Fig. 1b where enhanced fluctuations occur around narrow spikes centered at $k_x=2\pi/\Delta r_{rat}$ for n=5,10,15.

As noted previously, microtearing modes require the electron temperature gradient to surpass a threshold for instability to occur [7]. The linear threshold for the case here occurs at $a/L_{Te,th}\approx1.5$, well below the experimental gradient, $a/L_{Te,exp}\approx2.7$. Fig. 4 shows that the predicted transport is very "stiff", increasing 100% for an increase in a/L_{Te} of 20%, and approaching zero

for a 20% reduction. This stiffness suggests that, in locations where microtearing turbulence is active and dominant, profiles should adjust to be near marginal stability. Surprisingly, an effective non-linear threshold ($a/L_{Te,NL}\approx 2.1$) is apparent that is 40% higher than the linear threshold, reminiscent of the so-called "Dimits shift" in ITG turbulence [23]. Such a strong upshift has been observed before in finite-β ($\beta_e \leq 1\%$) simulations of ITG turbulence [18], although the reason for this remains unclear.

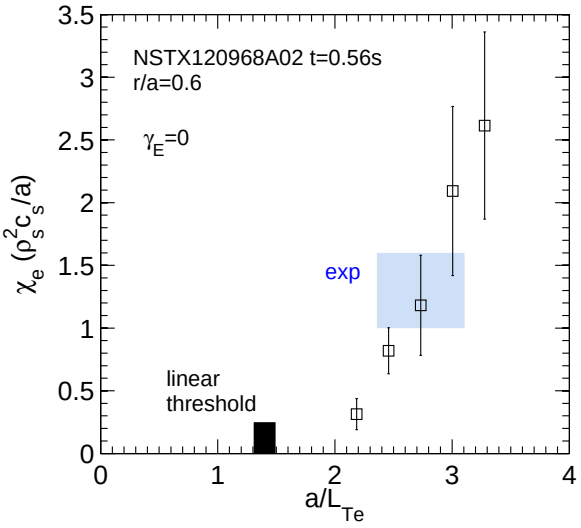

Fig. 4. Electron thermal transport vs. electron temperature gradient. Vertical bars represent statistical variation in the time-averaged transport. The shaded region represents the range of experimental uncertainty for χ_e and a/L_{Te}.

The above simulations do not include the finite toroidal flow and flow shear present in the neutral beam heated NSTX plasma. At r/a=0.6 the E×B shear rate, γ_E (defined in [24]) is comparable to the maximum linear growth rate of the microtearing modes, $\gamma_{E,exp}/\gamma_{lin,max}\approx 1.0$. Previous nonlinear simulations predict complete suppression of ITG and TEM turbulence for $\gamma_E/\gamma_{lin,max}\approx$1-2, depending on shaping and other parameters [25]. Unsurprisingly, the microtearing mode turbulence is largely suppressed when restarting the baseline simulation with the experimental value of γ_E. While this is now inconsistent with the experimental transport analysis at this location, the dependence in Fig. 4 suggests only a small increase in a/L_{Te} may be required to recover significant transport.

It is of great interest to measure turbulence characteristics in an attempt to correlate with the simulated microtearing expectations. Polarimetry measurements have been implemented in other tokamaks to measure δB fluctuations, and a system is being designed that may be sensitive to low-n δB perturbations in NSTX [26]. That the corresponding density perturbations at large poloidal wavelengths ($k_\theta \rho_s \leq 1$) are so narrow ($k_r \rho_s > 1$) (Figs. 1 and 2) also implies they may be detectable by the high-k coherent scattering diagnostic presently implemented on NSTX [27]. Regarding transport, the predicted ion thermal transport is negligible, expected for much slower ions in a stochastic magnetic field, and consistent with the experimental observation that χ_i is well described by neoclassical theory [1]. On the other hand, the stochastic field may contribute to the transport and redistribution of fast ions [28] present from neutral beam heating with large energies ($E_{i,fast}/T_e > 50$). Additional simulations are required to predict such transport from first principles.

In summary, this Letter presents first-of-a-kind non-linear microtearing mode simulations using comprehensive gyrokinetic simulations based on an NSTX discharge. The simulations require resolving all rational surfaces to achieve saturation, and the transport is almost entirely electromagnetic as a result of electrons diffusing in the stochastic magnetic field. The resulting electron thermal transport is comparable to experimental analysis, indicating microtearing modes can indeed cause significant transport in spherical tokamaks.

We gratefully acknowledge generous allocations at NERSC and resources of the Oak Ridge Leadership Computing Facility, supported by DOE contract DE-AC05-00OR22725. This work was also supported by DOE contracts DE-AC02-09CH11466, DE-FG03-95ER54309, and DE-AC52-07NA27344.

References

[1] S.M. Kaye et al., Nucl. Fusion **47**, 499 (2007).

[2] M. Valovič et al., IAEA, Daejon EXC/P8-18 (2010), submitted to Nucl. Fusion.

[3] J.F. Drake and Y.C. Lee, Phys. Fluids **20**, 1341 (1977).

[4] J.W. Connor, S.C. Cowley and R.J. Hastie, Plasma Physics Control. Fusion **32**, 799 (1990).

[5] F.M. Levinton et al., Phys. Plasmas **14**, 056119 (2007).

[6] D.J. Applegate et al., Plasma Phys. Control. Fusion **49**, 1113 (2007).

[7] K.L. Wong et al., Phys. Rev. Lett. **99**, 135003 (2007); K.L. Wong et al., Phys. Plasmas **15**, 056108 (2008).

[8] J. Wesson, *Tokamaks* (Oxford University Press, New York, 2004).

[9] G.M. Zaslavsky and B.V. Chirikov, Sov. Phys. Usp. **14**, 549 (1972).

[10] A.B. Rechester and M.N. Rosenbluth, Phys. Rev. Lett. **40**, 38 (1978).

[11] J.F. Drake, N.T. Gladd, C.S. Liu and C.L. Chang, Phys. Rev. Lett. **44**, 994 (1980).

[12] S.M. Kaye et al., Phys. Rev. Lett **98**, 175002 (2007).

[13] J. Candy and R.E. Waltz, Phys. Rev. Lett. **91**, 045001 (2003); J. Candy and R.E. Waltz, J. Comput. Phys. **186**, 545 (2003).

[14] J. Candy, Plasma Phys. Control. Fusion **51**, 105009 (2009).

[15] D. Applegate, Ph.D. Thesis, Imperial College London (2006).

[16] M. Kotschenreuther, G. Rewoldt and W.M. Tang, Comp. Phys. Comm. **88**, 128 (1995).

[17] P.H. Diamond, S.-I. Itoh, K. Itoh and T.S. Hahm, Plasma Phys. Control. Fusion **47**, R35 (2005).

[18] M.J. Pueschel, M. Kammerer and F. Jenko, Phys. Plasmas **15**, 102310 (2008); M.J. Pueschel and F. Jenko, Phys. Plasmas **17**, 062307 (2010).

[19] F. Jenko and W. Dorland, Plasma Phys. Control. Fusion **43**, A141 (2001).

[20] J. Candy, Phys. Plasmas **12**, 072307 (2005).

[21] E.Wang et al., Bull. Am. Phys. Soc. **55**, 193 (2010), submitted to Phys. Plasmas; W.M. Nevins, E. Wang and J. Candy, Phys. Rev. Lett **106**, 065003 (2011).

[22] R.W. Harvey, M.G. McCoy, J.Y. Hsu and A.A. Mirin, Phys. Rev. Lett. **47**, 102 (1981).

[23] A.M. Dimits et al., Phys. Plasmas **7**, 969 (2000).

[24] R.E. Waltz and R.L. Miller, Phys. Plasmas **6**, 4265 (1999).

[25] J.E. Kinsey, R.E. Waltz and J. Candy, Phys. Plasmas **14**, 102306 (2007).

[26] J. Zhang et al., Bull. Am. Phys. Soc. **55**, 45 (2010).

[27] D.R. Smith et al., Rev. Sci. Instrum **79**, 123501 (2008).

[28] T. Hauff, M.J. Pueschel, T. Dannert and F. Jenko, Phys. Rev. Lett. **102**, 075004 (2009).

The Princeton Plasma Physics Laboratory is operated
by Princeton University under contract
with the U.S. Department of Energy.

Information Services
Princeton Plasma Physics Laboratory
P.O. Box 451
Princeton, NJ 08543

Phone: 609-243-2245
Fax: 609-243-2751
e-mail: pppl_info@pppl.gov
Internet Address: http://www.pppl.gov